1. RESOLUTIONS AND SCALES

1.1 ATLAS detector response

As explained in chapter **??**, it is important to know detector scale and resolution in order to calculate corrections to the acceptance in terms of the geometrical cuts used in the event selection. For computation of differential quantities (for example, differential cross sections), detector response must also be folded in.

Detector scales and resolutions are represented in this analysis by what is known as a resolution function. From a Monte Carlo standpoint, this may be thought of, for variable x, as the distribution of x(Reco)-x(Truth) on an event by event basis. This chapter studies which resolution functions are of considerable size and methods of measuring resolution functions from data alone.

Table **??** summarises the required resolution functions [1] that are required for this analysis (taking into consideration the geometrical cuts used in the event selection). A summary of methods of determination is given, all of which are explained in more detail subsequently. The table states that an electron η resolution function is not required for the analysis. The reason is that, due to the high granularity of the ATLAS calorimeters, the angular resolution for an electron is neglible when compared to the momentum resolution, as may be seen in figure **??**. $\not{E}_t$ or electron resolution functions in terms of ϕ as no azimuthal cuts are used in the analysis.

Analysis	Object	Parameter	Method of determination
Z→ee	Electron	P_T	Z mass peak
W→eν	Electron	P_T	Z mass peak
Z→ee	Electron	η	Not necessary
W→eν	Electron	η	Not necessary
W→eν	$\not{E}_t$	P_T	- Neutrinofication from Z events - Axis resolution from Z events

Tab. 1.1: Resolution functions and data driven methods of determination

1.2 Electron response

The fractional MC resolution functions (Reco-Truth/Truth) for electrons are shown in figure **??**. The resolution is very clearly non-Gaussian, it has a large asymmetric lower side tail due to Bremsstrahlung radiation in the calorimeters as well as a high side tail due to bias from the selection cuts when making the resolution function. The angular resolution for electrons is

[1] Jets would be included in the case of a W/Z+jets cross section analysis but for an inclusive study this is not necessary

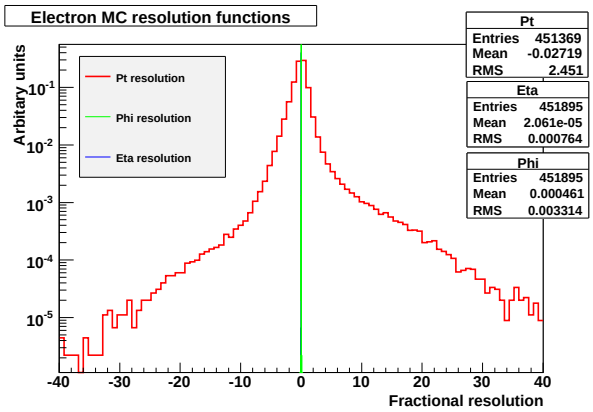

(a) Electron MC resolution functions

Fig. 1.1: Electron MC resolution functions

negligible when compared to the p_t resolution and thus will be neglected for the purposes of this analysis. It is necessary to study the resolution of the object with respect to its driving variable. Figure **??** shows how the mean and σ of the electron p_t resolution behaves with its p_t.

The electron resolution function will, in practise, be determined by studying the Z transverse mass peak, whose mean value and width are sensitive to the electron scale and resolution respectively. This has been studied in great detail by, in addition to other studies, the W mass ATLAS note **??**. The conclusion of this paper was that the expected systematic uncertainty on the electron scale and resolution using this method is 0.2% and 0.3% for the scale and resolution respectively, against which the statistical uncertainties are negligible (an order of 10 lower). These are the numbers assumed in the subsequent analysis.

1.3 $\not\!\!E_t$ response

1.3.1 $\not\!\!E_t$ in ATLAS

Computation

$\not\!\!E_t$ in ATLAS is, essentially, computed from the calorimeter energy deposits. The $\not\!\!E_t$ algorithms as well as the expected performance are described in **??**. The main $\not\!\!E_t$ reconstruction algorithm (RefFinal) is as follows:

Cell Based Method

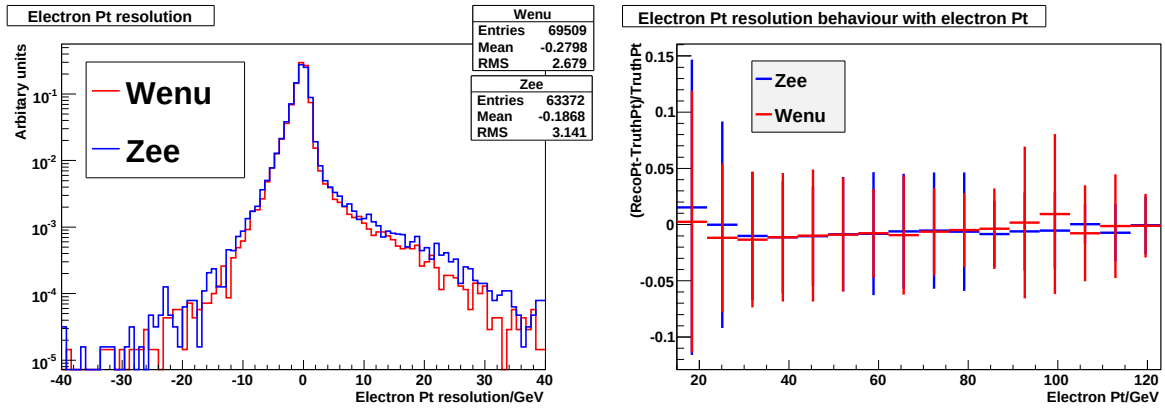

(a) Electron MC resolution functions

(b) Electron P_T resolution as a function of electron P_T

Fig. 1.2: Electron MC resolution functions

- A sum is made over energy deposit in calorimeter cells surviving noise cuts. Cells are initially calibrated using weights depending on their energy density.
- Corrections are made for reconstructed muons and energy lost in the cryostat.
- Cells are calibrated to the reconstructed object (electrons, taus, jets, muons) that they are assigned to (a global calibration is made for cells outside objects).

Performance

$\not{E}_t$ performance is evaluated in terms of linearity (scale) and resolution where those quantities are defined thus:

$$\text{Linearity} = \frac{\not{E}_t^{\text{true}} - \not{E}_t^{\text{reco}}}{\not{E}_t^{\text{true}}}, \tag{1.1}$$

$$\text{Resolution} = \sigma\left(\not{E}_{tx}^{\text{reco}} - \not{E}_{tx}^{\text{true}}\right) \tag{1.2}$$

where $_x$ denotes the $\not{E}_t$ resolved along a chosen axis, and σ refers to the width of the distribution in parenthesis. The $\not{E}_t$ resolution in both $Z \rightarrow ee$ and $W \rightarrow e\nu$ events is largely driven by the hadronic calorimeter resolution (the resolution contribution from the electrons is small compared with that from the hadronic deposits as shown later in the chapter). This is known **??** to scale with the energy deposit, E, in the calorimeters:

$$\frac{\sigma\left(\not{E}_t\right)}{E} = \frac{a}{\sqrt{E}} + b + \frac{c}{E}, \tag{1.3}$$

where the three terms in the equation are explained as follows:

- **a term:** Stochastic term. Originates from the statistical nature of the calorimeters and so follows a Poissonian distribution. Dominates in the middle energy region.
- **b term:** Constant term. Reflects the effect of the calorimeter non-compensation and the detector non-uniformitites involved in the energy measurement. Dominates at high energy.
- **c term:** Noise term. Due to the contribution of noise to the energy measurement. Dominates at low energies.

The $\not\!\!E_t$ in both $Z \rightarrow ee$ and $W \rightarrow e\nu$ events is in the region where the stochastic term dominates, and so the behaviour of $\not\!\!E_t$ with hadronic energy deposits is expected to follow the form

$$\sigma\left(\not\!\!E_t\right) = a\sqrt{E} + b. \tag{1.4}$$

In this analysis, $Z \rightarrow ll$ events are used to investigate techniques of understanding $\not\!\!E_t$ performance without relying on Monte Carlo truth. In an ideal detector no missing transverse energy would be seen in this channel and thus any missing energy seen in this analysis is a direct result of imperfections in the reconstruction process or the detector. This coupled with the clean event signature for a $Z \rightarrow ll$ event and its relatively large cross section mean that it is a good channel to study $\not\!\!E_t$. Two data driven techniques are studied in this thesis: axis resolution and neutrinofication. The application of these measured scales and resolutions to physics analyses are explored in greater detail in chapter **??**.

1.3.2 Axis resolution technique of $\not\!\!E_t$ resolution and scale determination

A particular axis defined from the event topology is defined, the reasons for the choice of which will become clear shortly. The axes will be used to resolve the $\not\!\!E_t$ along to check for resolution and biases. The axes used is the perpendicular (and its comparison- the parallel) axes, which are summarised in figure **??**.

Mathematically, the perpendicular bisector (which may then be normalised) is found by the following:

$$\mathbf{v}_{\perp} = \frac{\mathbf{Pt}_{e+}}{|Pt_{e+}|} + \frac{\mathbf{Pt}_{e-}}{|Pt_{e-}|} \tag{1.5}$$

where Pt_e are the momenta of the electron and positron. The parallel bisector is placed at $\frac{\pi}{2}$

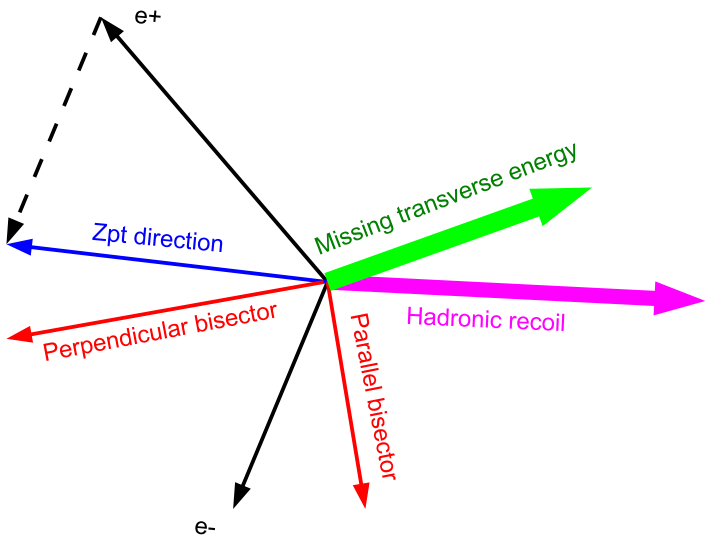

Fig. 1.3: ZPt direction, parallel and perpendicular bisectors in Z→ ee events

radians to the perpendicular.

Using axes to measure bias in MEt

A quantity that yields a measure of the $\not\!\!E_t$ scale is constructed. This is the mean of the distribution of the $\not\!\!E_t$ resolved along the perpendicular axis. If the $\not\!\!E_t$ computation in ATLAS is perfect, this value wil be zero in $Z \rightarrow ee$ events and so any deviation from zero suggests a bias in the MEt.

Figure **??** shows a profile plot (the so called 'Diagnostic plot') of such a quantity as the y variable, and the sum of the e+ and e- transverse momenta projected onto the perpendicular axis as the x variable (an indicator of the energy scale of the event; closely linked to the ZPt). This variable will be thought of as the hadronic recoil in the event. This plot may be used as a diagnostic tool, as this plot should, in theory, be a straight line through zero regardless of the energy of the lepton system.

The plot shows that, when resolved along the perpendicular axis, a clear bias in $\not\!\!E_t$ reaching down to about 7GeV is observed. Such a bias is not seen when the parallel axis is used. This can be explained by considering the event topology. The perpendicular axis is designed to be sensitive to the balance between the electrons and the hadronic recoil. The fact that the bias is

negative suggests that either the lepton system energy is being overestimated or the magnitude of the hadronic recoil underestimated. To distinguish between these two, the same plot was made with $Z \rightarrow \mu\mu$ events which can be observed in the right side of figure **??**. The same bias is seen, suggesting that the problem lies with the hadronic recoil. The parallel axis results are shown on the same plot as a sanity check. There is no such mechanism for bias using this axis and in this case a straight line through zero is seen.

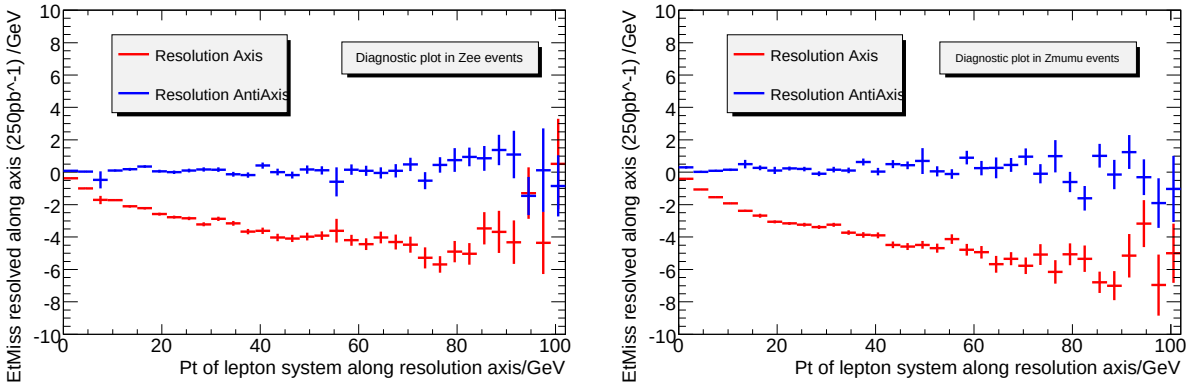

Fig. 1.4: Diagnostic plot compared when the $\not\!\!E_t$ is resolved along the parallel and perpendicular axis in $Z \rightarrow ee$ and $Z \rightarrow \mu\mu$ events.

Figure **??** shows the scale bias along the perpendicular or parallel axis with Monte Carlo comparison ($\not\!\!E_{t\ reco}$-$\not\!\!E_{t\ truth}$), and the large bias along the perpendicular is still clearly visible in the Monte Carlo. Thus the problem is in the ATLAS sofware and not to do with the methodology.

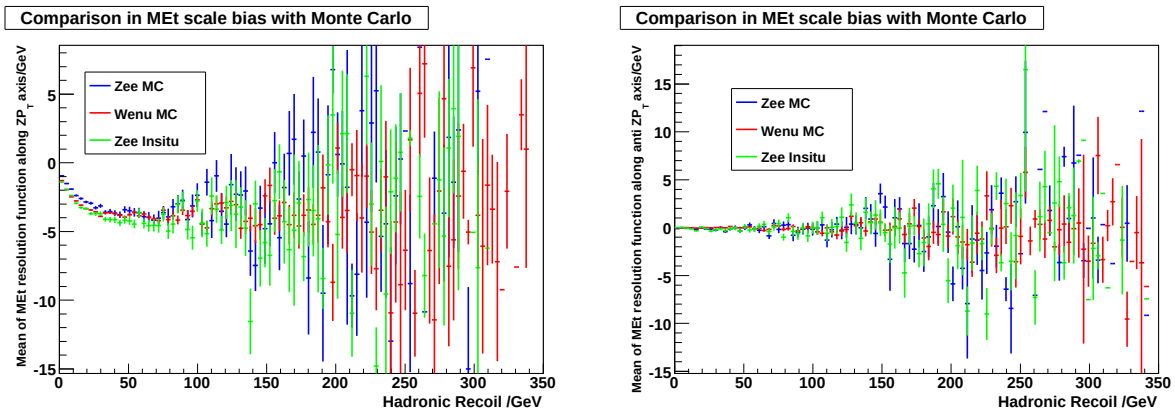

(a) Perpendicular (b) Parallel

Fig. 1.5: Diagnostic plot compared with Monte Carlo truth in both W and Z events.

Studies into the origin of this bias are currently underway. Figure **??** shows the energy of the real (truth) neutrinos in the event resolved along the axis. It shows that the contribution of real neutrinos to the bias is negligible. Figure **??** shows the diagnostic plot separated by jet multiplicity. It shows that the problem is worst in events with zero jets, which implies the problem lies with out of jet corrections. Another explanation is that the bias is due to particles losing too much energy in the upstream material so that they don't create any visible energy deposition in the calorimeter and at present the software makes no correction for this effect as it only applies correction factors to the energy deposition that is detected.
NOTE: more on this once the bias is fully understood.....

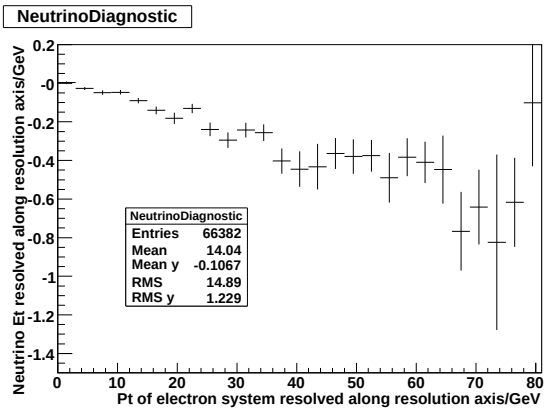

(a) Diagnostic plot made using truth neutrinos in the event

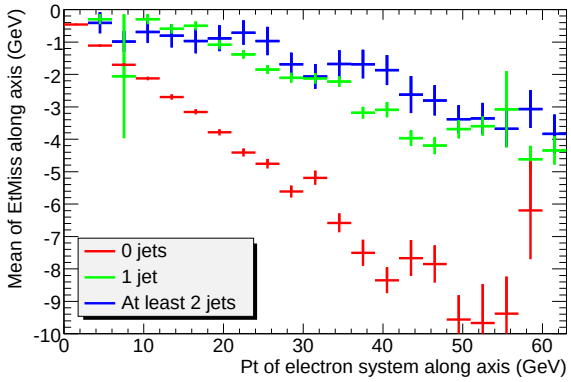

(b) Diagnostic plot split by jet multiplicity

Using axes to measure $\not\!\!E_t$ resolution

In the case of an ideal calorimeter, no missing energy would be seen in $Z \rightarrow ll$ events. Thus any missing energy that is 'detected' in the simulation must be a result of calorimeter imperfection and the spread of the distribution of the $\not\!\!E_t$resolved along an axis is interpreted as the calorimeter resolution. The question is which axis to use.

The ATLAS detector is capable of greater accuracy in angle measurement than in energy measurement. Thus an axis yielding an improved resolution may be one whose construction depends solely on the electron values of ϕ, and not their energies. Thus the axes to use are the parallel and perpendicular axes as these are constructed from the electron angles alone. Figure **??** shows the axis and $\not\!\!E_t$ resolution (from reco-truth) resolved along the parallel, perpendicular and ZPt directions. Figure **??** shows that a hugely improved resolution may be seen along the parallel and perpendicular axes (defined by electron angle alone) over that defined by the ZPt direction (defined by the electron angle and Pt). Figure **??** shows how this translates into an

$\not\!\!E_t$ resolution: the resolution along the parallel and perpendicular axes is better than that along the ZPt direction (NOTE: what about px???). It must be noted that the perpendicular axis has slightly better resolution than the parallel. This will be explained in a bit.

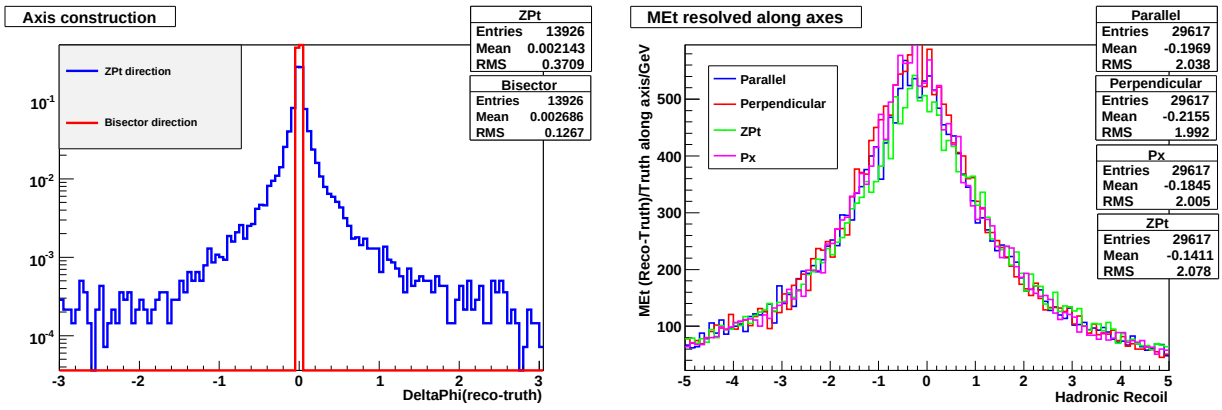

(c) Axis resolution (d) $\not\!\!E_t$ resolution

Fig. 1.6: Resolutions along the parallel, perpendicular, Px and ZPt direction

1.3.3 Parameterising $\not\!\!E_t$ resolution

If we recall that $\not\!\!E_t$is computed by summing up all energy in the x and y direction in the calorimeter, it is clear that the $\not\!\!E_t$ resolution is driven by the calorimeter resolution. This is dependent on the magnitude of the energy deposit and thus the $\not\!\!E_t$ resolution may be parameterised in terms of calorimeter activity. A further correction is made to facilitate direct comparison on an equal basis between Z events (2 electrons) and W events (1 electron) by subtracting off the electron contribution, which also makes sense as it is the hadronic activity which drives the calorimeter resolution. Hadronic activity is thus defined as:

$$\text{Hadronic Activity} = \sum Et - |P_{e+}| - |P_{e-}| \tag{1.6}$$

and in $Z \to \mu\mu$ events:

$$\text{Hadronic Activity} = \sum Et \tag{1.7}$$

where EtMissSum is the scalar sum of the energy deposits in the calorimeter cells. The distribution of hadronic activity for $Z \to ee$ and $W \to e\nu$ events is shown in figure **??**. The distributions in $Z \to ee$ and $W \to e\nu$ are very similar; the slightly higher values seen in the $Z \to ee$ sample than in the $W \to e\nu$ may be attributed to the slightly differing masses of the bosons.

Distributions in $\not\!\!E_t$along the resolution axis are taken in bins of hadronic activity in the event.

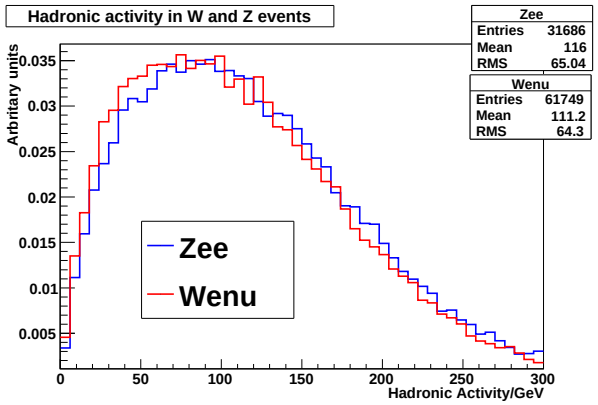

Fig. 1.7: Distribution of hadronic activity in $Z \rightarrow ee$ and $W \rightarrow e\nu$ events.

The behaviour of the RMS values of these distributions tells us how the calorimeter resolution behaves with its activity. The RMS values are shown in figure **??**. The plot shows what we would expect, as it is known that the resolution of a calorimeter worsens with energy. The fitted line is of the form

$$\sigma(MEt) = P_0\sqrt{\sum Et_{had}} + P_1 \tag{1.8}$$

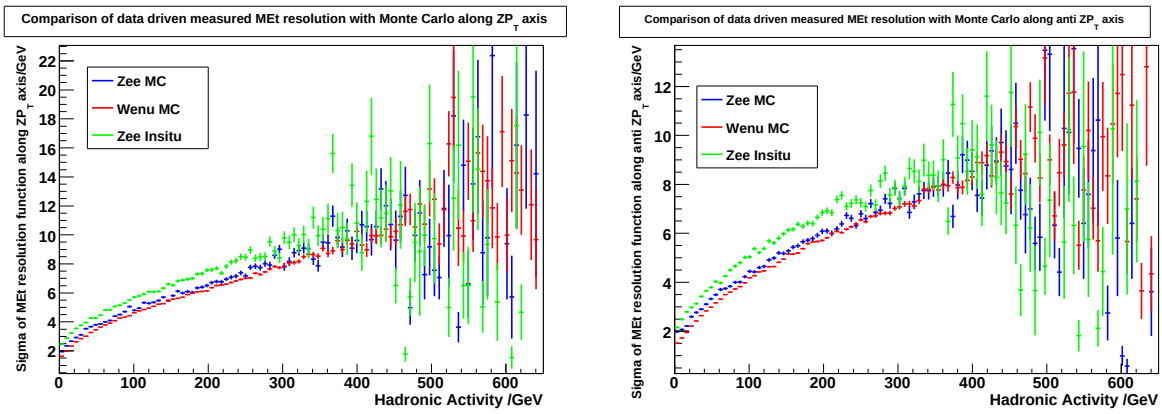

(a) Perpendicular axis

(b) Parallel axis

Fig. 1.8: $\not\!\!E_t$ Resolution functions along an axis obtained from resolving along axes. The Monte Carlo measured (Reco-Truth) resolution functions are shown by way of comparison.

As we have seen before in the global distributions, these values are smaller along the perpendicular axis than along the parallel exis. This is due to the contribution of the electron resolution to the analysis. Figure **??** shows the electron resolution (determined from Monte Carlo: reco-truth) along the parallel and perpendicular axes. It is seen that the electron reso-

lution contribution is much larger along the parallel axis than along the perpendicular. This is because, as an artifact of the axis construction, the electron component is largest along the parallel and smallest along the perpendicular. It is known that, in an opposite effect as for muons, the electron resolution increases with electron p_t and thus the resolution along the parallel will be in fact maximised along the parallel and minimised along the perpendicular. This could be a measure of determining electron resolution from data alone. Figure **??** shows the $\not\!\!E_t$ resolution along each axis before and after the electron resolution is subtracted off in quadrature. We see that after the subtraction, the resolution along the perpendicular and parallel now agree as the only effect left is that of hadronic resolution, which ought to be the same along both axes.

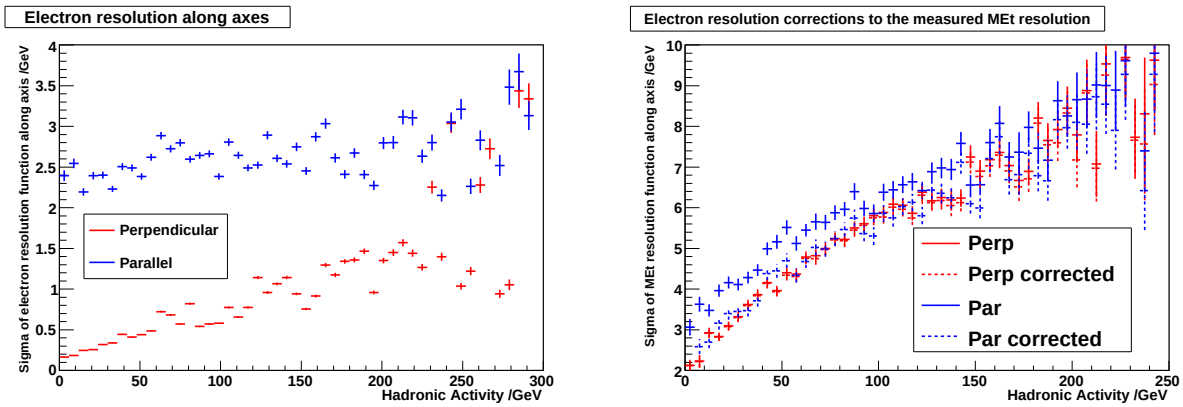

(a) Electron resolution along parallel and perpendicular axes

(b) Impact of electron resolution on measured $\not\!\!E_t$ resolutions

Fig. 1.9: Comparison in resolutions with muonic events.

Comparison with different samples

The same analysis was done on the Z→ee+jet and Z→ $\mu\mu$ samples and the results shown in figure **??**. All graphs agree showing that the method is consistent in different samples.

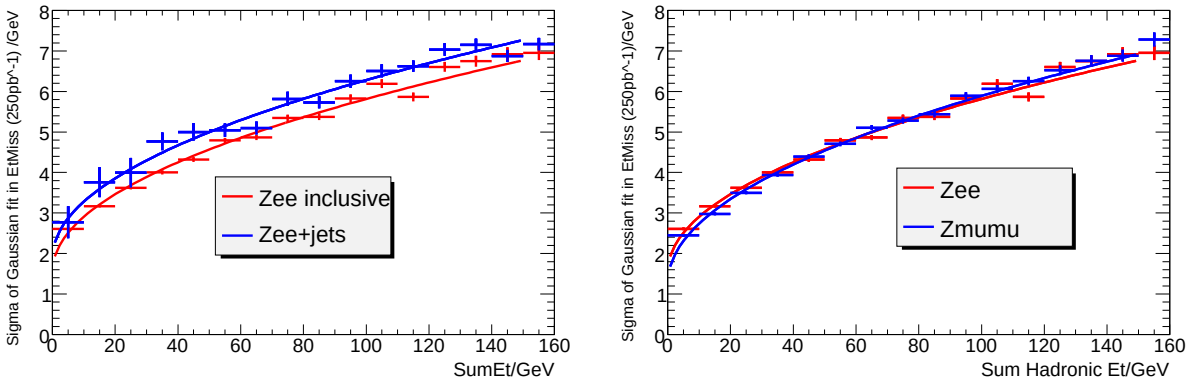

Fig. 1.10: Profile plots of $\sigma(\mathbf{Et}_{miss})$ against $\sum \mathrm{Et}_{had}$ in Z→ee+jet and Z→ $\mu\mu$ events.

1.3.4 Data driven $\not\!\!E_t$ resolution functions- neutrinofication technique

Using neutrinofication to measure $\not\!\!E_t$ resolution

This is an alternative method of measuring $\not\!\!E_t$ resolution in ATLAS without relying on Monte Carlo. The technique hinges on the fact that W and Z are actually very similar processes except, to a good approximation, that one of the electrons from a Z event is equivalent to a neutrino in a W event. $\not\!\!E_t$ scales and resolutions in a W event may be approximated by those in a Z event if one of the electrons is 'neutrinofied', that is, if the event is treated as if the electron was a neutrino as may be seen in figure **??**.

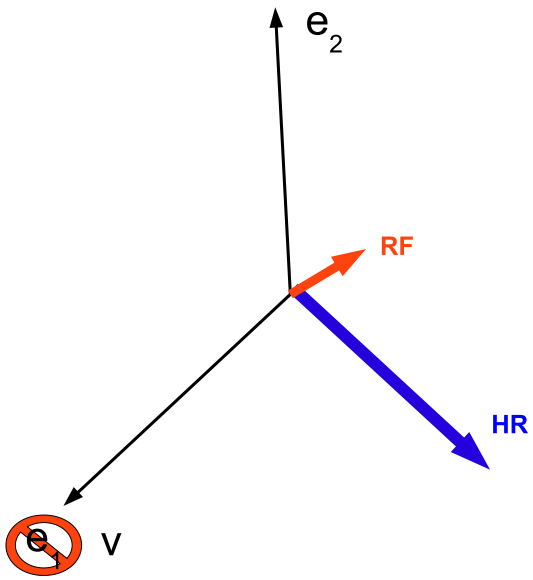

Fig. 1.11: Neutrinofication of a Z event. RF is the reconstructed ('RefFinal') $\not\!\!E_t$ in the event, and HR refers to the hadronic recoil.

In the case of neutrinofication, the truth $\not\!\!E_t$ vector is taken to be:

$$\mathbf{\not\!\!E_t}^{truth} = \mathbf{e_1}^{reco}. \tag{1.9}$$

Note this involves the assumption of perfect electron resolution with respect to the $\not\!\!E_t$ resolution. If this Z event was in fact a W event, the reconstructed $\not\!\!E_t$ vector would be found to

be the negative vector sum of all other activity in the event, that is to say:

$$\mathbf{\not{E}_t}^{reco} = -1 \times (\mathbf{e_2}^{reco} + \mathbf{HR}) \tag{1.10}$$

The vector quantity, hadronic recoil is not present in standard ATLAS AODs. Happily however, it is possible to calculate it using the negative sum of all other objects in the event, that is:

$$\mathbf{HR} = -1 \times (\mathbf{e_1}^{reco} + \mathbf{e_2}^{reco} + \mathbf{RF}), \tag{1.11}$$

and thus we have

$$\mathbf{\not{E}_t}^{reco} = \mathbf{e_1}^{reco} + \mathbf{RF}. \tag{1.12}$$

Now we have both 'truth' and 'reconstructed' $\not{E}_t$ in the 'W' event, resolution functions of the form reco-truth may be measured from purely reconstructed quantities. Given that these are all vector sums, resolution functions, $\mathbf{R}$, in terms of both p_t and ϕ may be obtained. The resolution function in terms of p_t is given by the distribution of the following:

$$\mathbf{R} = |\mathbf{e_1}^{reco} + \mathbf{RF}| - |\mathbf{e_1}^{reco}|, \tag{1.13}$$

and is shown shown in figure **??**. The agreement is seen to be poor when global p_t resolution is studied.

However working out the maths for the p_t resolved along the perpendicular and parallel axes we see that

$$\mathbf{R}_\perp = (\mathbf{e_1}^{reco} + \mathbf{RF})_\perp - \mathbf{e_1}_\perp^{reco} = \mathbf{RF}_\perp \tag{1.14}$$

and similar for the parallel. This is the same the distributions obtained by just resolving the reconstructed $\not{E}_t$ in the event along the axes! Thus the distributions have already been shown in figure **??** and good agreement is observed.

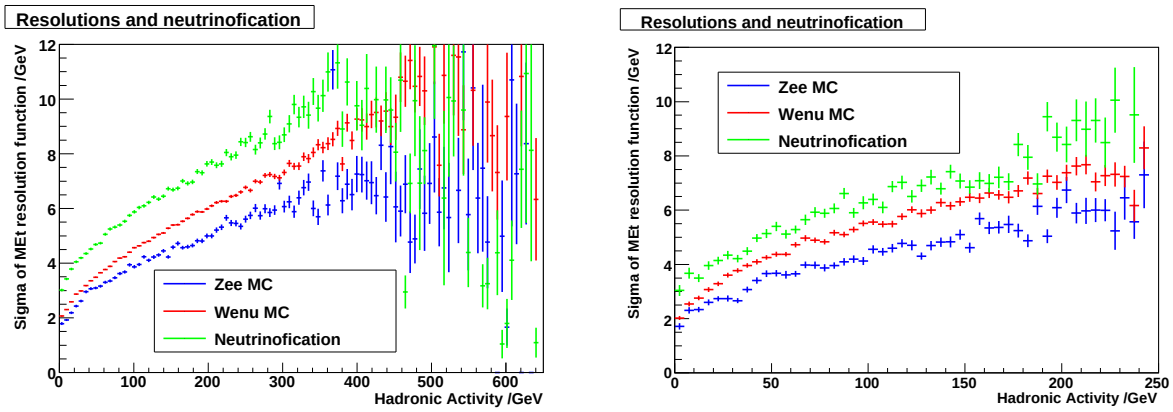

(a) Global neutrinofication (b) Binned neutrinofication

Fig. 1.12: $\not\!\!E_t$resolution function obtained from neutrinofication of a Z event. The Monte Carlo measured (Reco-Truth) resolution functions are shown by way of comparison.

Using neutrinofication to measure bias in MEt

Following the logic in the preceeding section, we see that the bias plots in terms of hadronic recoil will be the same as for the axes technique. However neutrinofication has an added advantage over simply using axes to resolve the observed $\not\!\!E_t$ in the event along. It will become clear in the next chapter that it is necessary to bin $\not\!\!E_t$ scale in terms of $|\not\!\!E_t|$ itself. Obviously this creates a problem in Z analysis as there is very little $\not\!\!E_t$ to bin in! However in neutrinofication it is possible to bin in terms of the 're-reconstructed' $\not\!\!E_t$ as defined by equation **??**. Figure **??** shows such distributions with a fourth order polynomial fit. To explain briefly the plot, we see two elements:

- Large positive bias at low $\not\!\!E_t$. This is a consequence of construction: at truth $\not\!\!E_t$ (x value) =0, reconstructed $\not\!\!E_t$ will be forced to be larger than truth $\not\!\!E_t$ as it can't be negative. Thus the y value $\not\!\!E_{t\ reconstructed}$-$\not\!\!E_{t\ truth}$ will be forced to be positive.
- bias becomes steadly lower and falls negative at higher $\not\!\!E_t$. This is due to the way the Jacobian peak smears out but is as of yet not fully understood. (NOTE: Need to do something about this).

1.4 Estimation of uncertainties

The uncertainties obtained are those on the global resolution functions.

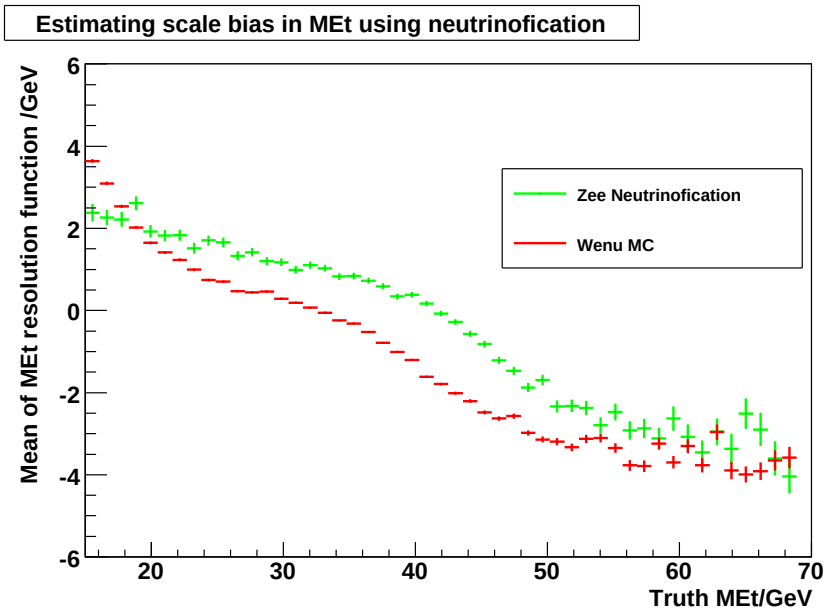

Fig. 1.13: $\not\!\!E_t$ scale as a function of the size of —$\not\!\!E_t$— itself obtained from neutrinofication of a Z event. The Monte Carlo measured (Reco-Truth) resolution function is shown by way of comparison. The fit shown is a fourth order polynomial.

1.4.1 Statistical

The statistical uncertainty on the mean, $\epsilon(\overline{x})$, and resolution, $\epsilon(\sigma)$, of a resolution function with N entries, mean $\overline{x}$ and RMS σ are given, by the central limit theorem:

$$\epsilon(\overline{x}) = \frac{\overline{x}}{\sqrt{N}}, \tag{1.15}$$

and,

$$\epsilon(\sigma) =? \; CHECKTHIS. \tag{1.16}$$

It is assumed the statistical errors on $\overline{x}$ and σ are similar for both MC and data driven methods, as these result in very similar distributions. The resultant statistical errors on the parameters are summarised in table **??**.

Object	Analysis	$\epsilon(\overline{x})$/GeV	$\epsilon(\sigma)$/GeV
Electron	$Z \rightarrow ee$	0.014	0.010
Electron	$W \rightarrow e\nu$	0.011	0.008
$\not\!\!E_t$	$W \rightarrow e\nu$	0.025	0.018

Tab. 1.2: Statistical errors on scales and resolutions

1.4.2 Systematics

Systematic errors on the scale and resolution are determined by taking the average bin-by-bin deviation between those quantities determined insitu and in the Monte Carlo truth distributions. The number of bins used to determine the average is truncuated at the point where statistical fluctuations become large. The systematic error on the procedure of smearing truth values to compute acceptances is determined separately in chapter **??**. The systematic uncertainties on the scale and resolution for the $\not\!\!E_t$resolved along and perpendicular to the Z P_T (denoted variable a) are estimated by the following:

- Systematic estimator 1 (%) = $a_{Insitu} - a_{ZMC}$W
- Systematic estimator 2 (%) = $a_{Insitu} - a_{WMC}$

The systematic estimators on $\overline{x}$ and σ obtained are summarised in table **??**. It must be noted that for some quantites (scale along the anti Z P_T direction) the percentage uncertainties are artifically large as the quantity is centered around zero and in this case the absolute uncertainty is more informative.

Estimator	$\epsilon(\overline{x})$/GeV (ZP_T direction)	$\epsilon(\overline{x})$/GeV (anti ZP_T direction)	$\epsilon(\sigma)$/GeV (ZP_T direction)	$\epsilon(\sigma)$/GeV (anti ZP_T direction)
1	-0.48 (8.8%)	-0.034 (151.89%)	0.72 (9.7%)	0.54 (7.5%)
2	-0.22 (3.3%)	-0.07 (11.1%)	0.97 (13.0%)	0.78 (11.9%)
Overall	5%	100%	10%	10%

Tab. 1.3: Systematic estimators on scales and resolutions. Absolute estimators are given with percentage estimators in parenthesis.